www.lpr-journal.org

LASER & PHOTONICS REVIEWS

WILEY-VCH

WILEY ONLINE LIBRARY

Early View publication on wileyonlinelibrary.com
(issue and page numbers not yet assigned;
citable using Digital Object Identifier – DOI)

LASER & PHOTONICS REVIEWS

Laser Photonics Rev., 1–11 (2013) / **DOI** 10.1002/lpor.201300103

Abstract The wavelength dependence of the nonlinear absorption and the third order nonlinear refraction of crystalline silicon between 2.75 μm and 5.5 μm as well as at 1.55 μm have been measured. It was found that at all wavelengths multi-photon and free carrier absorption can be significant. In particular nonlinear absorption can affect silicon devices designed for the mid-infrared that require strong nonlinear response, such as for the generation of a supercontinuum.

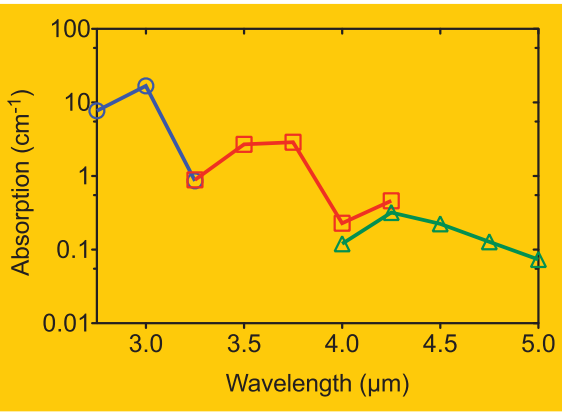

ORIGINAL PAPER

Nonlinear absorption and refraction in crystalline silicon in the mid-infrared

Xin Gai[1], Yi Yu[1], Bart Kuyken[2], Pan Ma[1], Steve J. Madden[1], Joris Van Campenhout[4], Peter Verheyen[4], Gunther Roelkens[2,3], Roel Baets[2], and Barry Luther-Davies[1,*]

1. Introduction

Silicon is increasingly becoming the dominant photonic material for signal processing, optical sensing and lab-on-a-chip [1–3]. However, it is well known that silicon displays significant two-photon absorption (2PA) in the telecommunications band centred at 1.55 μm [4, 5] and this places a limit on the utility of silicon waveguides for ultrafast signal processing in telecommunications using third order nonlinear optics. The nonlinear figure of merit, $F = n_2/\beta_{2PA}\lambda$ where n_2 is the nonlinear refractive index and β_{2PA} is the two-photon absorption coefficient, determines the maximum nonlinear phase shift that can be achieved in a waveguide device. For silicon $F \approx 0.3 - 0.4$ at 1.55 μm. Whilst this is large enough for silicon waveguides to be used for signal processing based on four-wave mixing, it is too small for strongly nonlinear processes, for example, optical switching or supercontinuum (SC) generation for which $F > \pi$ is required. Furthermore, free carriers are generated by 2PA and these add to the total absorption, although this can be mitigated, to some extent, by reducing the carrier lifetime either by recombination at surfaces [6] or in the bulk for ion implanted samples [7]; or by sweeping the carriers from the waveguide using a p-i-n structure [8, 9].

There have been a number of measurements of n_2 and β_{2PA} for silicon for wavelengths between ≈1.2 μm and 2.3 μm [4, 5, 10]. These authors used very similar techniques and samples, but reported a range of values for n_2 between $\approx 2.3 - 5.5\times10^{-5}$ cm^2/GW and $\beta_{2PA} \approx 0.45 - 0.8$ cm/GW at 1.55 μm. In theory 2PA should become negligible once the photon energy becomes less than half the optical gap corresponding to wavelengths beyond ≈ 2.2 μm. Whilst measurements showed a large reduction in 2PA by 2.2 μm they did not demonstrate that the nonlinear absorption completely disappeared. More recently Pearl et al. [11] measured three-photon absorption (3PA) in silicon between 2.3 μm and 3.3 μm and showed it was significant with a maximum 3PA coefficient, $\beta_{3PA} \approx 0.035$ cm^3/GW^2 at ≈2.8 μm. 3PA would be expected to become negligible beyond about 3.3 μm, however, the experimental data did not unequivocally confirm this.

Based on such results it has been widely claimed that in the mid infrared, beyond the cut-off for 2PA, silicon becomes a very good third order nonlinear material and this prediction appears to have been confirmed in recent experiments. Kuyken et al. [12] showed that a supercontinuum could be generated in a silicon waveguide by pumping with 2ps duration 2.12 μm pulses and, very recently, Lamont et al. [13] reported successful SC generation in

[1] Centre for Ultrahigh bandwidth Devices for Optical Systems, Laser Physics Centre, Research School of Physics and Engineering, The Australian National University, Canberra ACT2600, Australia
[2] Photonics Research Group, Department of Information Technology, Ghent University IMEC, Ghent B-9000, Belgium
[3] Center for Nano- and Biophotonics (NB-Photonics), Ghent University, Ghent, Belgium
[4] IMEC, Kapeldreef 75, Leuven B-3001, Belgium
*Corresponding author : e-mail: barry.luther-davies@anu.edu.au

a dispersion engineered silicon waveguide pumped using ≈300 fs pulses around 2.5 μm. Hence, on the face of it, nonlinear absorption in silicon appears not to be serious in the mid-IR.

In this paper we explore the nonlinear optical properties of silicon focusing particularly on the mid infrared from 2.75 to 5.5 μm where currently measurements are absent. We find that n_2 changes very little as the wavelength increases within this range but more importantly that the nonlinear absorption never disappears. We show that the recent experiments on mid-IR SC generation in silicon [12, 13] were performed with experimental parameters where the effects of nonlinear absorption were relatively small. However, with slightly different experimental conditions, very strong nonlinear absorption would have occurred and this would have prevented SC generation. We demonstrate this in the following section where we attempted experiments to generate a mid-IR SC using very similar waveguides to those of Lamont et al. [13] but where longer pulses were employed.

This paper is organised as follows. Firstly, we describe experiments aimed at mid-IR SC generation in dispersion engineered silicon waveguides which motivated us to measure nonlinear absorption in silicon at long wavelengths. We then describe those measurements and discuss the difficulties that are encountered when trying to determine the order of the nonlinear absorption. Since we found it was essential to include free carrier effects we include measurements of the nonlinear properties of silicon at 1.55 μm from which an accurate value of the free carrier absorption coefficient was obtained which was then used in analysis of the mid-IR data. Finally, we present the results of measurements of the refractive and absorptive nonlinearities in silicon in the mid-IR and discuss the consequences for experiments, such as SC generation, that require strong nonlinear response.

2. Mid-IR experiments in SOI waveguides

The results of Kuyken et al. [12] motivated us to try and extend the SC generated from a silicon waveguide up to the limit due to absorption for a silicon-on-insulator (SOI) device at 4.2 μm, much further than the maximum of 2.5 μm achieved using the 220 nm × 900 nm waveguides employed in [12]. According to simulations, this required both a longer wavelength pump and a change of the waveguide structure to shift the zero dispersion region further into the mid-IR. Thus, we used a 400 nm thick Si layer and calculated that the zero dispersion wavelength shifted from 1.8 μm to beyond 2.9 μm as the waveguide width was increased from 1.3 μm to 1.85 μm.

Centimetre-long samples were fabricated using the 200mm CMOS line at IMEC. The waveguides were up-tapered to a width of ≈8 μm at the input and output to improve coupling. The optical losses had been measured previously to be $\leq 3dB/$ cm at 3.8 μm [14]. We note that 1.8 μm waveguides wide have a significantly lower nonlinear parameter, γ ($= 2\pi n_2/\lambda A_{eff}$ where A_{eff} is the area of the waveguide mode) compared with those used in [12]

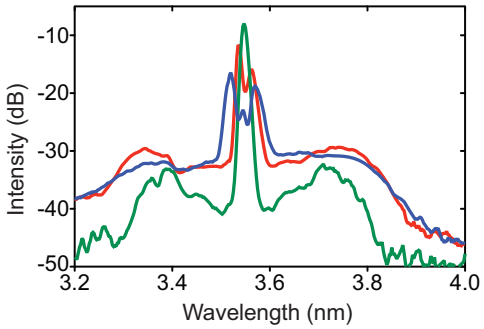

Figure 1 Spectra at the output of a 1.8 μm wide waveguide pumped with 3.55 μm pulses with peak power in the waveguide of ≈ 50 W (green); ≈ 100 W (red) and ≈ 250 W (blue).

because of the longer pump wavelength but also because the mode area is larger. For a pump at 3 μm we calculated γ to be ≈ 9 $W^{-1}m^{-1}$ assuming a value for $n_2 \approx 3\times10^{-14}$ cm^2/W. This meant that the power required for processes like SC generation increases to several hundred watts compared with only ≈12.7 W for the 2.12 μm pump [12].

To generate a SC, pulses at 1.5MHz repetition rate from a mid-IR optical parametric amplifier (OPA) [15] tunable from 3 μm-5 μm were coupled into the waveguides using molded chalcogenide lenses. The focal spot at the input was measured to be between 3 μm and 4 μm in diameter by imaging it with a NA = 0.85 molded lens onto an InSb camera. The waveguide output was imaged onto the input slit of a Newport Cornerstone 0.25 m monochromator fitted with a PbSe detector. The details of the experimental arrangement were very similar to those reported in [16]. Significant in what follows was the fact that the pulse duration from the OPA was 7.5 ps and that the maximum single pulse fluence at the input facet reached 0.2 J/cm^2.

Initially we measured the evolution of the output spectrum with increasing input power. As the power increased the spectrum broadened due to self-phase modulation and the background noise around the pump (caused by fluorescence from our high gain OPA) was amplified as expected by parametric amplification (Fig. 1) indicating the onset of the modulational instability: a precursor to SC generation. However, as the input was further increased, the broadening no longer increased proportionally and, in fact, it became apparent that the total output power was no longer increasing. This pattern repeated for all input wavelengths within the transparency range of the waveguide (up to 4.2 μm). As a consequence we decided to measure the intensity dependence of the waveguide output obtaining the results shown in Fig. 2(a).

Figure 2(a) shows that initially the output rose almost linearly with input but once a threshold was passed, corresponding to pulse intensities ≈5 GW/cm^2 at the input facet, there was an abrupt and very considerable drop in transmission. Very clearly a nonlinear process was clamping the waveguide transmission. At the highest intensities we could also damage the tapers at the waveguide input. When this occurred the damage was restricted to a region

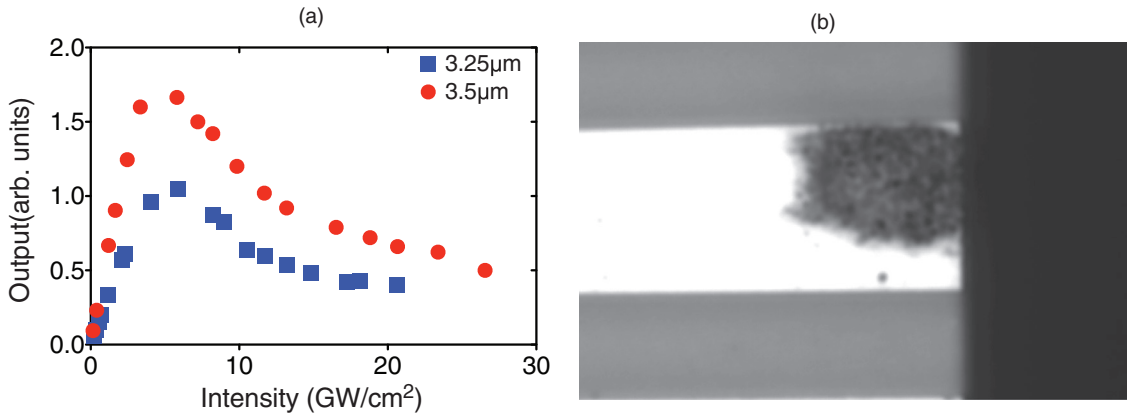

Figure 2 (a) Output vs input intensity at the waveguide facet for 1.7 μm wide SOI waveguides pumped at 3.25 μm and 3.5 μm; (b) a microscope image of damage at the input facet looking down onto the waveguide from above. The waveguide had been up-tapered to 8 μm width at its input. The damages extended around 8 μm into the waveguide

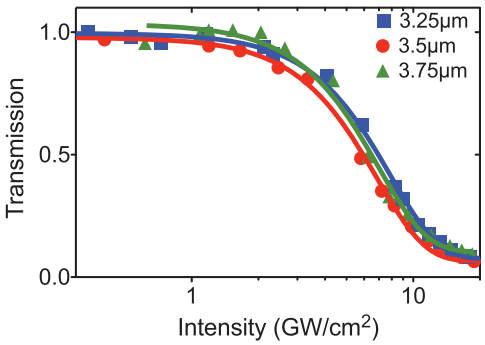

Figure 3 Nonlinear transmission vs intensity at the input facet for a 1.7 μm wide SOI waveguide at 3.25 μm, 3.5 μm and 3.75 μm. The lines are Gaussian fits which, whilst they fit the data very well, are only included only as guides for the eye.

≈5 μm wide, smaller than the taper width (see Fig. 2(b)). From curves such as those in Fig. 2(a) we calculated the intensity dependence of the normalised (to the value at low intensity) transmission and this is shown for three wavelengths in Fig. 3. These curves again illustrate the sudden switch-on of absorption since the transmission remained close to unity until a threshold was passed after which it dropped to as low as 10%. This behaviour is inconsistent with a single multi-photon absorption process acting alone since it would result in a more gradual change in transmission with intensity, especially when time-averaging is taken into account.

Whilst it is not the purpose of this paper to provide a complete quantitative explanation of these waveguide measurements, we found in our simulations where we solved the nonlinear Schrödinger equation using the split step Fourier method that it was necessary to include three and/or four photon absorption, free carrier absorption (FCA) and additionally electron avalanche multiplication to obtain curves that even remotely reproduced the experiments.

Logically in the wavelength band between 3 μm and 4 μm, 4PA would be the dominant multi-photon process. However, to our knowledge, there have, so far, been no measurements of the 4PA absorption coefficients for silicon and even the values for 3PA are not known very accurately beyond 3 μm [11]. Hence we could only estimate the values for these multi-photon absorption coefficients by fitting the simulations to the experiments. However, once a small level of multi-photon absorption occurs, free carriers are generated and these have an important effect because the FCA increases with λ^2 [17, 18]. However, whilst including reasonable estimates for 3PA and 4PA coefficients and including FCA, predicted that the output would saturate and then start to drop, the calculations failed to reproduce the dramatic reduction of output shown in Fig. 2(a).

Recall, however, that the single pulse fluence at the input facet reached $0.1 - 0.2$ J/cm^2 and this was sufficient to damage the silicon. According to Pronko et al. [19] and Vaidyanathan et al. [20] this fluence is enough to cause electron avalanche multiplication, a process associated with optical damage in silicon. The avalanche breakdown threshold decreases with increasing wavelength, that is, avalanche multiplication requires low intensities at long wavelengths. Thus, we added electron avalanche multiplication to our code and this rapidly increased the free carrier density once a certain threshold was exceeded somewhat improving the trends compared with the experiment. Hence, our best qualitative explanation of Figs. 2(a) and 3 is that electron avalanche multiplication dominates the interaction. At low fluence there are too few electrons to seed the avalanche process and, hence, the free carrier density remains low and the absorption is negligible. The material can be thought of as "biased" by the AC field into a pre-breakdown state. Once sufficient seed electrons have been generated by four-photon absorption, the electron avalanche takes off and this results in a step increase in the free carrier density causing a precipitous drop in transmission.

The points to take from this are that, firstly, it is not safe to ignore the effects of high order multi-photon and

free carrier absorption in silicon in the mid-IR, at least in some experimental conditions. Secondly, since the free carrier lifetime greatly exceeds the pulse duration the number of free carriers increase with the pulse fluence and, hence, long pulses will create more seed electrons than short ones. Hence, for the same maximum intensity, free carrier effects should be less of a problem with fs compared with ps pulses. This qualitatively explains why the experiments reported by Lamont et al. [13] on supercontinuum in waveguides pumped with 300 fs pulses were successful but ours using 7.5 ps pulses were not. In what follows we attempt to quantify the nonlinear absorption from transmission measurements on a wafer of intrinsic silicon for wavelengths between 2.75 μm and 5.5 μm.

3. Nonlinearity and multi-photon absorption in bulk silicon

In order to quantify the higher order effects we measured the nonlinear absorption and refraction in a 500 μm thick double side polished (100) intrinsic silicon wafer. Whilst our main focus was the mid-IR, we also include a set of measurements we had performed at 1.55 μm which we used to obtain as accurate a value as possible for the free carrier absorption coefficient.

Our experiments used pulses generated by a Quantronix Palitra OPA pumped by a Clark MXR CPA2001 Ti:sapphire laser operating at 1 kHz. In the near-IR the signal output was used for z-scan measurements. The mid-IR beams were obtained by difference frequency mixing between the signal and idler outputs and this generated 2−5 mW of average power at wavelengths between ≈2.75 μm and 5.5 μm. After appropriate filtering to remove either the idler for the near-IR measurements or both the signal and idler for the mid-IR, the beam was truncated with an aperture to improve its spatial coherence and focused using a 10 cm focal length CaF_2 lens into the sample. Because of residual aberrations and aperturing, images of the beam using an InSb camera showed that about 80% of the power was contained in the central spot. The pulse durations in the mid-infrared were found to be 190 ± 20 *fs* from autocorrelation measurements using two-photon absorption in an InGaAs detector with an extended IR response to 2.6 μm.

Two slightly different methods of recording the data were employed in near-IR and mid-IR experiments respectively. In the near-IR the beam transmitted through the sample was imaged using a Xenics InGaAs camera and a series of frames were captured as the sample was translated through the focus. This data was then post processed to extract open and closed aperture z-scans.

To determine the nonlinearity as well as two-photon and free carrier absorption coefficients requires careful analysis of both open and closed aperture z-scans using models that accurately extract the relevant coefficients from the experimental data. In addition it is normally necessary to know with accuracy the pulse and beam parameters of the source used in the measurements to obtain absolute values for nonlinearity and absorption coefficients. To check we had correct values for the experimental parameters at 1.55 μm, our z-scan measurements were "calibrated" using a material whose nonlinearity is known accurately and where there is no nonlinear absorption to contend with. We used As_2S_3 as this reference material since its nonlinearity had been measured accurately by self-phase modulation in waveguides and found consistently to have a value of $2.9 \pm 0.3 \times 10^{-14}$ cm^2/W [21].

In the mid-IR the beam transmitted through the sample was imaged using a 50mm focal length CaF_2 lens onto a PbSe detector. A similar detector monitored the input to the sample using the surface reflection from a CaF_2 beam splitter. An aperture at the imaging lens could be closed to convert the detected signal from open to closed aperture configuration. The closed aperture signal was also used to determine the peak-to-valley distance, Z_{p-v}, and the relation $Z_{p-v} = 1.7\,\pi\omega_o^2/\lambda$ where ω_o is the Gaussian electric field radius, to determine the beam size. We found that the beam area was essentially independent of wavelength and had the value $\pi\omega_o^2 = 6.6\times10^{-5}$ cm^2.

By closing the aperture at the imaging lens and translating the sample along the beam axis, we obtained closed aperture z-scans which could be used to determine the nonlinear refractive index, n_2. This was carried out at 500 nm intervals between 3 μm and 5.5 μm. At each wavelength several traces were obtained for different intensities allowing ΔT_{p-v} to be determined as a function of intensity after normalisation to the relevant open aperture trace. The slope of the curve at zero intensity was used to determine the nonlinear refractive index.

We then proceeded to make the intensity dependent transmission measurements. Two sets of measurements were made at each wavelength: one with the sample in the focus and one with it well away from the focus to check the linearity of the detectors. To record a data set, the intensity incident on the sample was varied by slowly rotating the first of a pair of wire grid polarisers positioned in the input beam. Data was logged automatically as the intensity was varied under computer control. Examples of the raw data are shown in Fig. 4(a). The results of measurements of the transmission as a function of input intensity and wavelength are shown in Fig. 4(b). To obtain these curves a large number of data points representing the output versus input were first fitted using high order polynomials. The transmission was then determined using the fitted curves rather than the raw data. This proved to be the best way to reduce noise from the transmission measurements which otherwise relied on division of two small signals contaminated by noise near zero intensity to define unity transmission. An example of the raw data and fitting curves is shown in Fig. 4(a) corresponding to the curve for 4.0 μm in 4(b) shown as the dashed curve.

It is worth noting that the beam was polarised along the (110) axis of the silicon for these measurements. We did observe slight anisotropy in the absorption similar to that reported in [11] if the sample was rotated around its (001) axis, however, the change in absorption was only a few tens of percent and would not change the values of

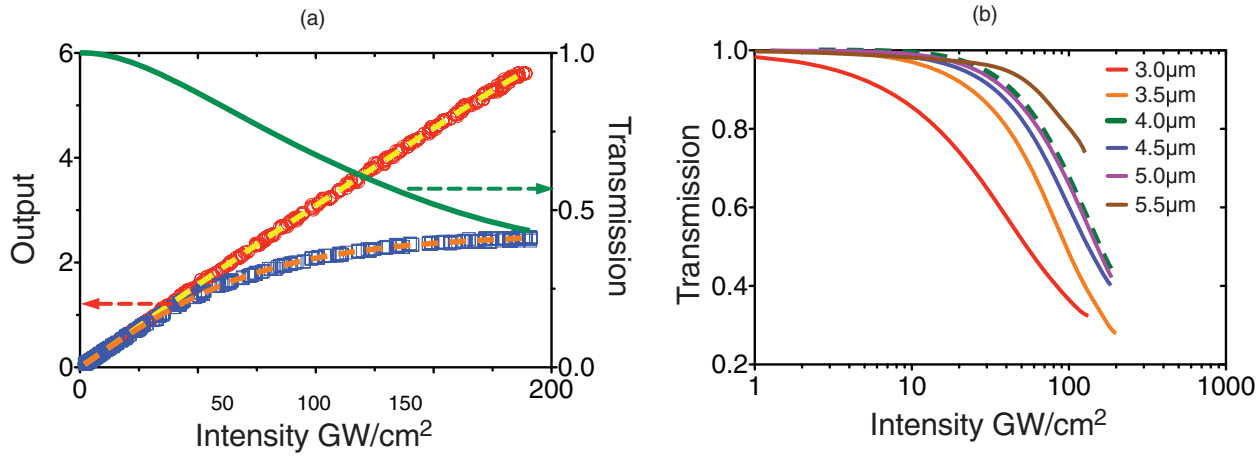

Figure 4 (a) Illustration of the procedure used to obtain the transmission data (Fig. 4(b)). Two sets of data were taken at 4.0 μm the first with the sample in focus (blue) and the second out of focus (red). The data was then fitted with sixth order polynomials (yellow and orange dashed lines) constrained to have the same slope at zero intensity. The resulting curves were then divided to obtain the transmission shown as the green line. (b) Measured transmission for wavelengths between 3 μm and 5.5 μm at 0.5 μm intervals.

the absorption coefficients to within the accuracy of the experiments.

4. Nonlinear properties at 1.55 μm

The data collected in the mid-IR has to be analysed to extract the levels of both free carrier and multi-photon absorption. This is complicated by the fact that more than one multi-photon process may be present and due to uncertainty in the value of the free carrier absorption coefficient. These difficulties are reduced in the near-IR where only 2PA should be present and where free carrier effects are relatively well understood. Nevertheless, values for the third order nonlinearity and β_{2PA} determined from almost identical experiments by different authors still differ by more than a factor of 2 [4, 5, 10] and this also places some uncertainty on the level of free carrier absorption. As a result we decided to analyse our z-scan measurements at 1.55 μm in detail to extract n_2, β_{2PA} and the free carrier absorption coefficient, σ_{FCA}.

There are several possible factors, apart from experimental uncertainties, that could account for discrepancies between values obtained by different authors using nominally identical experiments. The first factor is the use of a simplified model to fit the experimental z-scan data [4, 10, 22]. When $\beta_{2PA} = 0$ this model is a good approximation even for relatively large values of nonlinear phase change. However, as 2PA increases the functions are only accurate when $\beta_{2PA} I L_{eff} \ll 1$. From our analysis we find that the error is around 5% when $\beta_{2PA} I L_{eff} = 0.1$, and 13% when $\beta_{2PA} I L_{eff} = 0.2$. In materials like silicon, As_2Se_3, and III-V semiconductors which display relatively strong 2PA, this implies the measurements must be made at low intensities and in such conditions the data becomes contaminated by noise which makes it difficult to obtain accurate estimates of either n_2 and β_{2PA}. A second factor that can introduce errors is the assumption that FCA is negligible but this is not the case, even with ultrashort pulses, when high intensities are used to reduce the effects of the noise.

An accurate z-scan model was provided in the original work of Sheik-Bahae et al. [23], however, this formalism does not include the effects of FCA. Furthermore, the generation rate for the free carriers depends on the local instantaneous beam intensity but, because the carrier lifetime is much longer than the pulse duration, the number of free carriers accumulates over the pulse and is, therefore, proportional to the fluence. Thus, it is not possible to develop a simple analytic model to describe the effect of free carriers for even the open aperture z-scan signal. Thus we resorted to numerical techniques to analyse the open aperture data. Since we operated in the "thin sample" regime we could neglect diffraction and self-focussing but included the effects 2PA and absorption due to the free carriers created by 2PA at a rate given by:

$$\frac{\partial N(z,r,t)}{\partial t} = \frac{2\pi\beta_{2PA} I(z,r,t)^2}{2h\omega} - \frac{N(z,r,t)}{\tau} \qquad (1)$$

where $N(z, r, t)$ is the radial and time dependent carrier density at a particular distance, z along the z-scan direction corresponding to a beam intensity $I(z, r, t)$.

Open aperture data was recorded over a range of intensities up to ≈ 30 GW/cm^2 and the scans fitted with numerical models including only 2PA or both 2PA and FCA. Examples of the fitted curves are show in Fig. 5(a,b) for two different intensities. As is evident, whilst at low intensity the open aperture curves are well-fitted by 2PA alone as the intensity increases past about 10 GW/cm^2 FCA has to be added to fit the experimental data. Fig. 5(c) plots the measured variation of 1/T as a function of intensity compared with the calculated variation for 2PA alone (red curve) and

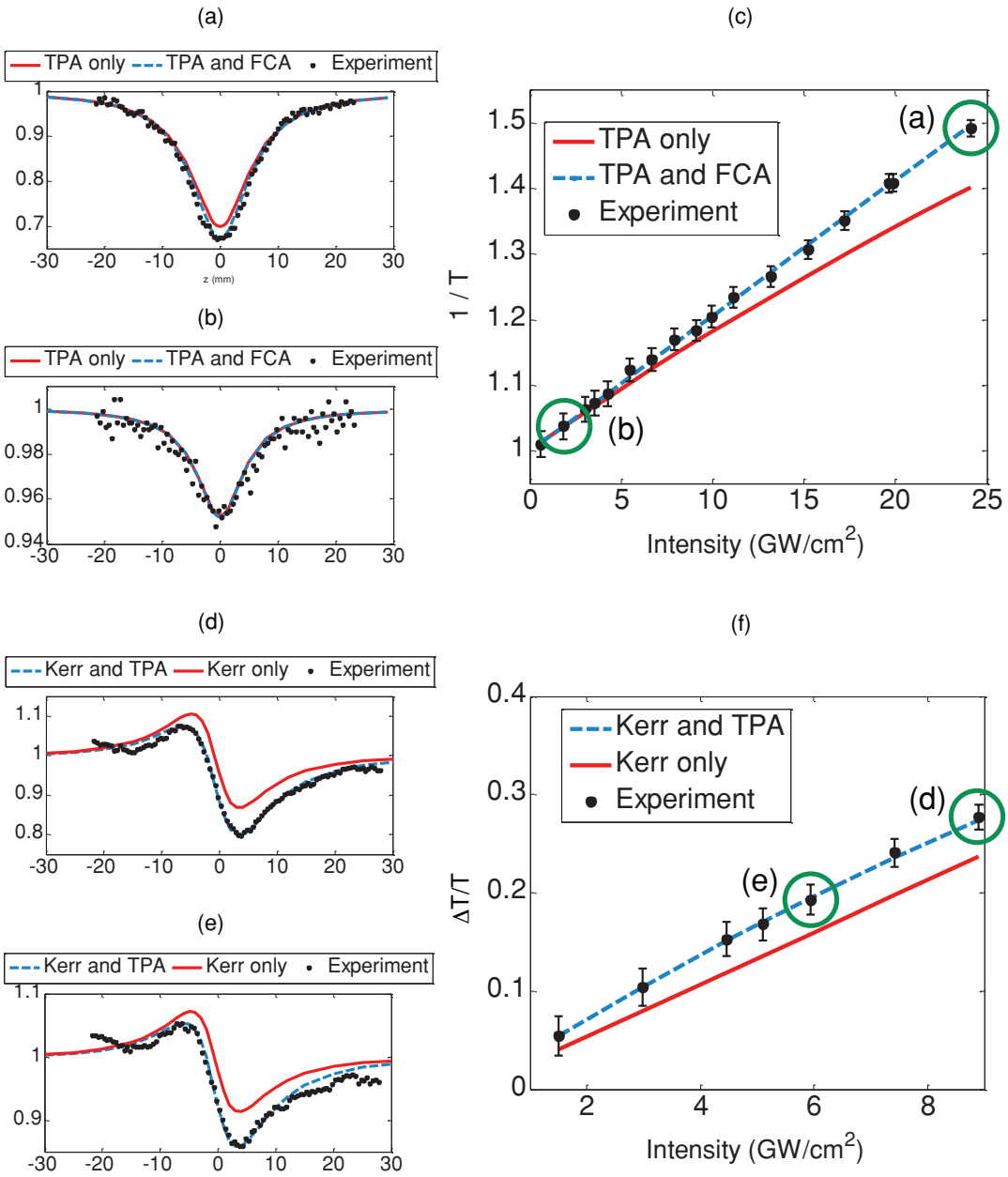

Figure 5 (a,b) Open aperture z-scans recorded at 1.55 μm at the two intensities circled in green are shown in 5(c). The black dots are the experimental data; the red line is a curve fit using 2PA alone and the blue dashed lines are curve fits including both 2PA and FCA. 5(c) Inverse transmission is plotted as a function of maximum intensity with fits to 2PA alone and 2PA plus FCA. 5(d,e) Closed aperture z-scans recorded at 1.55 μm at the two intensities circled in green in 5(f). The black dots are the experimental data; the red line is a curve fit using 2PA alone and the blue dashed lines are curve fits including both 2PA and FCA. 5(f) ΔT/T is plotted as a function of maximum intensity with fits to 2PA alone (red line) and 2PA plus FCA (blue dashed line).

including 2PA and FCA (blue dashed curve). This shows it is essential that FCA is included to obtain a satisfactory fit over the full intensity range. From these data we obtain β_{2PA}, of 1.03×10^{-11} m/W and $\sigma_{FCA} = 1.45 \times 10^{-17}$ cm^2. It is worth noting that our value for σ_{FCA} is consistent with that obtained by Boggess et al. [27], Schroder et al. [28] and Svantesson [29] assuming that σ_{FCA} scales proportional to λ^2. In additional our value is consistent with that reported by Cutolo et al. at 1.55 μm.

From Fig. 5(c) we found that FCA is insignificant at intensities <10 GW/cm^2 and, hence, we could analyse the closed aperture traces using the full z-scan model descibed by Sheik-Bahae [23] in this range. Figure 5(d,e) shows fits to the experimental data based on the Kerr nonlinearity combined with 2PA (blue dashed line) and without 2PA (red line). Figure 5(f) demonstrates an excellent fit is obtained using the value of β_{2PA} deduced from the open aperture trace and with $n_2 = 6.7 \pm 0.6 \times 10^{-14}$ cm^2/W.

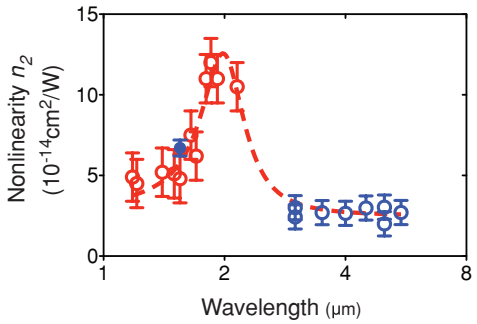

Figure 6 Measured third order nonlinearity, n_2, at infrared wavelengths combining our results (in blue) with those of Bristow [4] (red). The dotted line is a Lorentzian fit used simply as a guide for the eye.

5. Nonlinear properties in the mid-IR

The values we found for n_2 versus wavelength in the mid-IR are shown in Fig. 6 where we have also added the data from [4] for the near-IR and our measurement at 1.55 μm. We found that between 3 and 5.5 μm the nonlinearity dropped only very slightly with wavelength and had an average value around $2.7 \pm 0.5 \times 10^{-14}$ cm^2/W. This is qualitatively consistent with the results of Dinu [24] who predicted that for $\hbar\nu/E_{ig} \approx 0.2 - 0.3$ the nonlinearity changes quite slowly with wavelength, here E_{ig} is the indirect band gap of silicon and ν the frequency. Our value for n_2 at 1.55 μm lies within the range reported by Bristow et al. [4], so combining their results and ours suggests that the nonlinearity peaks at 1.2×10^{-13} cm^2/W at 1.8 μm before then dropping progressively to $\approx 3 \times 10^{-14}$ cm^2/W at 3 μm.

6. Analysis of the transmission experiments

Figure 4(b) demonstrates that at all wavelengths the transmission decreased with increasing intensity and, in general, it decreased earlier for the shorter wavelengths. This confirmed that nonlinear absorption indeed occurred, and the issue now becomes how to analyse these results to extract the multi-photon (and free carrier) absorption.

Several authors have discussed the analysis of transmission measurements to determine high order nonlinear absorption demonstrating that this is a far from trivial task once spatial and temporal averaging over the pulse and beam profiles have been taken into account [23, 25]. The main difficulty arises from the fact that after such averaging the transmission curves for different orders of nonlinear absorption become very similar. The main approach has been to plot the inverse transmission $(1/T)^{n-1}$ against intensity I^{n-1} since this should produce a linear relationship only for a specific value of n: the order of the multi-photon absorption. Unfortunately, spatial and temporal averaging also means that the linear region only exists for very small deviations of the transmission from unity ($1/T < 1.1$) [25] and in our experiments even using hundreds of data points and averaging, noise contaminated the data in this range. Thus, the best approach appeared to compare the overall shape of the complete curves to calculations. There are, however, some additional complications: firstly, free carrier absorption needs to be taken into account and, secondly, at some wavelengths contributions to the absorption can occur from both n-photon and $(n+1)$-photon processes simultaneously. Wherrett [26] provided simplified scaling curves for direct-gap semiconductors which demonstrated this, however, to our knowledge similar results are not available for indirect gap materials like silicon except for 2PA [10]. Nevertheless, based on Wherrett's results, around 3 μm one might expect both 3PA and 4PA; around 4 μm both 4PA and 5PA; and around 5 μm both 5PA and 6PA. As a result we could only fit our data to models of 3-, 4-, 5- and 6-photon absorption assuming that only the single most likely multi-photon process occurred at each wavelength and from this estimate the multi-photon absorption coefficients.

To model the transmission behaviour we used the same computer code used to calculate 2PA at 1.55 μm modified for n-photon absorption and including FCA. To quantify the absorption due to free carriers we used the value of $\sigma_{FCA}(1.55\ \mu\text{m}) = 1.45 \times 10^{-17}(\text{cm}^2)$ extracted from the z-scan at 1.55 μm and scaled this to longer wavelength using the relation $\sigma_{FCA}(\lambda) = \sigma_{FCA}(1.55\ \mu\text{m}) \times (\lambda(\ \mu\text{m})/1.55)^2$.

In Fig. 7(a-c) we show examples of measured and calculated transmissions corresponding to different orders of nonlinear absorption and for several different wavelengths. The values of the nonlinear absorption coefficients obtained from the fitted curves are tabulated in Table 1 and include uncertainties from two sources. Table 1 estimates the uncertainty due to the standard errors from least squares fitting of theoretical curves to our data. In addition there is an uncertainty of about ± 15% in the absolute values of the intensity. In this latter case the uncertainty in the absorption coefficient depends on the order of the multi photon process. For 3PA the uncertainty is (−28%, +32%); for 4PA it becomes (−40%, +60%;) and for 5PA it is (−50%, +75%). With these uncertainties in mind, we found that at 4.5 μm, a convincing fit to 5−photon absorption was obtained with an estimated absorption coefficient of $1.4 \pm 0.4 \times 10^{-6}$ cm^7/GW^4. At 3.75 μm a very good fit was obtained to 4-photon absorption with a coefficient of $3.6 \pm 0.9 \times 10^{-4}$ cm^5/GW^3. By 2.75 μm the fit is reasonable to 3-photon absorption with a value of $2 \pm 0.5 \times 10^{-2}$ cm^3/GW^2. In the regions around 4μm and 5 μm the fits were somewhat poorer whilst at 5.5 μm no satisfactory fit could be obtained to the anticipated 6-photon absorption.

In Figs. 7(d-f) we have plotted the calculated nonlinear transmission using the values for the n-photon absorption coefficient from Table 1 at 3 μm, 4 μm and 5 μm with and without FCA. These demonstrate that FCA is significant in all conditions of these experiments. Depending on the wavelength, FCA increases the absorption by $\approx \times 1.25$ at 3.0 μm and $\approx \times 2$ at 5 μm: that is FCA gets bigger at the longer wavelengths. Taken in conjunction with the data of Fig. 8, short pump wavelengths are preferable to minimise FCA and operating at 3.25 μm should result in the lowest total nonlinear absorption.

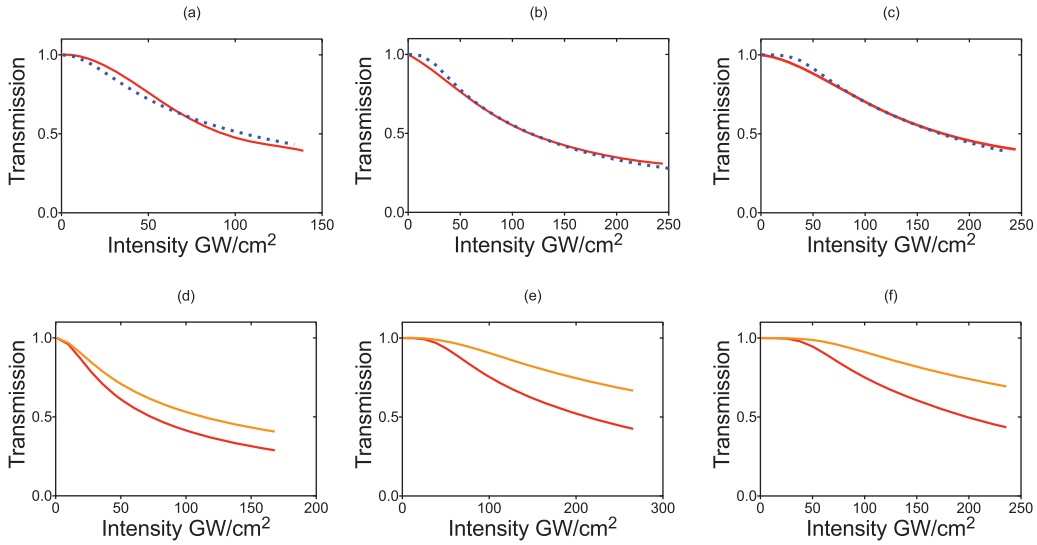

Figure 7 (a) Experimental data (red) and fitted curve (blue dotted) for 3PA at 2.75 μm; (b) Experimental data (red) and fitted curve (blue dotted) for 4PA at 3.75 μm; (c) Experimental data (red) and fitted curve (blue dotted) for 5PA at 4.5 μm; (d) A comparison the predicted absorption with both FCA and 3PA (red) and 3PA alone (orange) at 3.0 μm; (e) A comparison the predicted absorption with both FCA and 3PA (red) and 4PA alone (orange) at 4.0 μm; (f) A comparison the predicted absorption with both FCA and 3PA (red) and 5PA alone (orange) at 5.0 μm;

Table 1 Nonlinear absorption coefficients. The values in red correspond to the expected dominant n-th order nonlinear absorption at a particular wavelength, whilst those in black represent the value assuming the (n-1)th order absorption occurred.

Wavelength (μm)	β_3(cm^3/GW^2)	β_4(cm^5/GW^3)	β_5(cm^7/GW^4)	β_6(cm^9/GW^5)
2.75	$2.0 \pm 0.5 \times 10^{-2}$	-	-	-
3.0	$4 \pm 1 \times 10^{-2}$	-	-	-
3.25	$2 \pm 0.5 \times 10^{-3}$	$1 \pm 0.25 \times 10^{-4}$	-	-
3.5	-	$3.5 \pm 0.9 \times 10^{-4}$	-	-
3.75	-	$3.6 \pm 0.9 \times 10^{-4}$	-	-
4.0	-	$3 \pm 0.75 \times 10^{-5}$	-	-
4.25	-	$6 \pm 1.5 \times 10^{-5}$	$2 \pm 0.5 \times 10^{-6}$	-
4.5	-	-	$1.4 \pm 0.4 \times 10^{-6}$	-
4.75	-	-	$8 \pm 4 \times 10^{-7}$	-
5.0	-	-	$5 \pm 1.3 \times 10^{-7}$	-
5.25	-	-	$1.6 \pm 0.4 \times 10^{-7}$	-
5.5	-	-	poor fit $\approx 7 \times 10^{-8}$	poor fit

The numbers in Table 1 might, on initial inspection, seem rather small. However, take the value at 3.75 μm as an example. In a waveguide the absorption coefficient due to nonlinear absorption will be roughly 10 dB/cm at 14 GW/cm^2. For the waveguide used in our experiments the mode area at 3.75 μm was ≈0.83 μm^2 and hence this corresponds to 116W in the waveguide. Using this power, the nonlinear phase shift can be calculated to be < 3 radians.

Within the wavelength range where each n-photon process is expected to operate, the data indicates that there are maxima in the values of the coefficients at ≈ 3 μm for 3PA; ≈ 3.75 μm for 4PA and ≈ 4.25 μm for 5PA. These are qualitatively consistent with the scalings predicted by Wherrett [26] for direct gap semiconductors. This suggests there may be "sweet spots" for experiments. This is illustrated in Fig. 8 where we plot the relative absorption due to 3PA, 4PA and 5PA versus wavelength for an intensity of 20GW/cm^2. As is evident the loss is smallest around 3.25 μm and 4 μm and beyond about 4.75 μm. Since the nonlinearity, n_2 is not changing much across this wavelength range, significantly larger nonlinear phase change can be expected by operating near these minima.

7. Discussion

Our results demonstrate that nonlinear absorption exists in silicon across a major part of its transparency range. Just over a four-fold increase in intensity is all that is needed

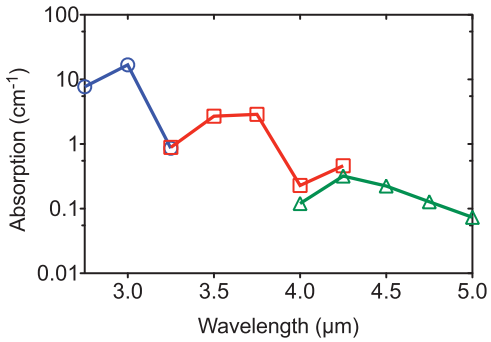

Figure 8 Calculated loss using the values from Table 1 for three (blue), four (red) and five (green) photon absorption for an intensity of 20GW/cm^2 as a function of wavelength

to reach the same absorption from 5PA at 5 μm as was obtained by 3PA at 3 μm. On the basis of Table 1 we can see that the absorption coefficients generally decrease with increasing wavelength. The trouble is, however, that they do not drop fast enough to compensate for the increasing scaling with intensity since a 5PA process, for example, the absorption coefficient increases with I^4 and, thus, a relatively small increase in intensity is all that is required to recover a high level of absorption. In addition the FCA is strong at long wavelengths.

This has a serious consequence for some waveguide devices since as we move further into the infrared the intensity required to achieve a specific nonlinear phase change inevitably increases in proportion to wavelength and inversely with nonlinearity. As evident in Fig. 6, n_2 does not change very much between 3 μm and 5 μm but on the basis of these and Bristow's results [4] between 2 μm and 3 μm, the nonlinearity drops by a factor of 3-4 so the intensity required to produce the same nonlinear phase shift increases by more than a factor of 5 over this range. The end result is that the nonlinear absorption remains strong if a large value of nonlinear phase shift must be generated as is the case for SC generation. For other processes where the required nonlinear phase shift is smaller, for example those based on four wave mixing, nonlinear absorption can be avoided provided the maximum intensity is limited, for example, by using a long device.

Nonlinear loss is, therefore, not always dominant as evidenced by the successful experiments of Lamont et al. [13]. If we compare Figs. 3 and 4(b) we can see that reducing the pulse duration from 7.5 ps to 250 fs increases the threshold for strong absorption by about an order of magnitude. Clearly this suggests that short pulses will be essential to achieve strong nonlinear effects. Of course in these two examples the propagation length was also quite different (1cm *c.f.* 0.05 cm) and this alone could affect the observed absorption. To clarify this we modelled the transmission of a 1 cm long waveguide assuming a linear loss of 3 dB/cm pumped at a wavelength of 3.25 μm with pulses of 300 fs, 1 ps, 3 ps and 10 ps and plot the power-dependent transmission in Fig. 9. We considered two cases: one corresponding to a situation where the waveguide dispersion was

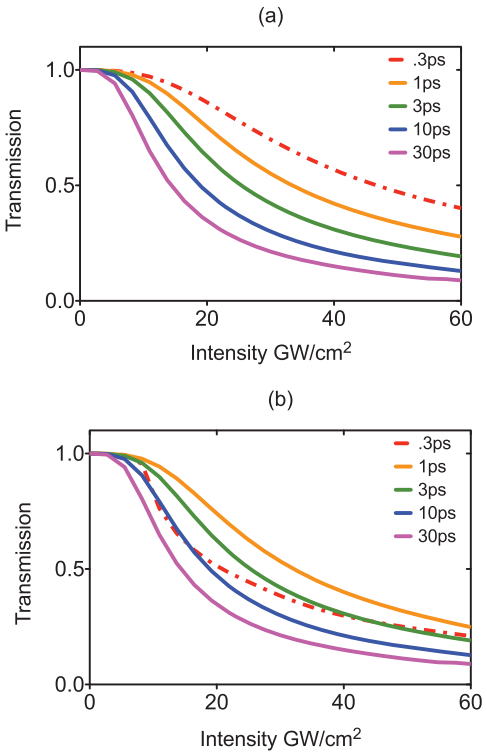

Figure 9 Calculated transmission for 1cm long, 1.8 μm wide ×0.4 μm thick air clad silicon waveguide pumped at 3.25 μm with different pulse durations assuming a 4PA absorption coefficient of 1×10^{-4} cm^5 GW^3 and FCA. (a) Normal dispersion of 0.54 ps^2/m; (b) anomalous dispersion of −0.54 ps^2/m. The case of the 300 fs pulse is highlighted using the dot dashed line in red.

normal, and the second when it was anomalous. For these simulations we used a numerical code to solve the nonlinear Schrödinger equation using the slit-step Fourier method including the effects of linear as well as high order nonlinear absorption and free carrier absorption but neglecting avalanche multiplication.

In the case of normal dispersion in Fig. 9(a) the absorption starts at lower and lower powers as the pulse duration is increased. For the shortest pulse the free carrier contribution is very small and hence high intensities can be used limited only by 4PA. However, as the pulse gets longer the free carrier concentration accumulates during the pulse leading to a marked increase in absorption. For a 30 ps duration pulse the transmission drops by 3 dB at about 14 GW/cm^2 compared with about 60 GW/cm^2 at 300 fs. These results qualitatively confirm the trends from Figs. 3 and 4(b).

The case of anomalous absorption is an interesting one and is shown in Fig. 9(b). In this case the trends for Fig. 9(a) are repeated for the pulses of 1 ps or longer but in the case of the 300 fs pulse 3 dB absorption occurs at about half the intensity compared to the case of normal dispersion. We can understand this behaviour by examining the pulse dynamics as it propagates along the waveguide. Pulses <1 ps in duration, undergo compression and soliton fission, that is the soliton fission length becomes

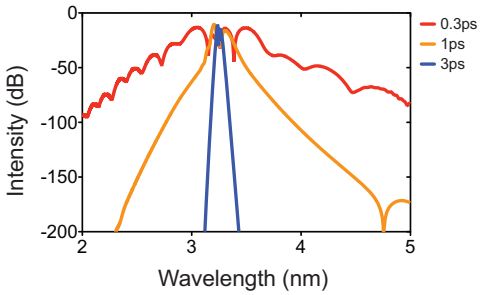

Figure 10 Simulated output spectra for a 1 cm long, 1.8 μm wide ×0.4 μm thick air clad silicon waveguide for different pulse durations assuming 4 PA absorption coefficient of 10^{-4} cm^{5}GW^3 and FCA for anomalous dispersion of -0.54 ps^2/m. The input power was 153 W, 235 W and 185 W at 0.3 ps, 1 ps and 3 ps respectively which corresponds to the powers that produce 3 dB of nonlinear loss in the waveguide at each pulse duration.

less than the device length. As this occurs the local pulse intensity rises due to pulse compression above the input intensity and this has the effect of enhancing the nonlinear absorption. At the same time this means that the spectrum has broadened. This is illustrated in Fig. 10 where we plot simulated spectra for three different pulse durations using input intensities which lead to 3 dB of nonlinear loss. What is very clear here is that the spectrum is significantly broadened for the shortest pulses suggesting that SC generation is possible in this regime.

Of course reducing the intensity required to achieve a strong nonlinear response will always help reduce the impact of a high-order multi-photon process. This can be achieved by increasing the device length, provided of course the linear losses are small enough. In our current waveguides the losses were up to 3 dB/cm and this needs to be reduced to perhaps 1 dB/cm to usefully increase the effective device length, L_{eff}.

8. Conclusions

In this paper we present the first measurements of the third order optical nonlinearity of silicon as well as the multi-photon absorption coefficients in the mid-IR. We find that the third order nonlinear refractive index averages $2.7 \pm 0.5 \times 10^{-14}$ cm^2/W between 3 μm and 5 μm changing very little with wavelength. This compares with the value we also measured at 1.55 μm of 6.7×10^{-14} cm^2/W, which is within the range reported by Bristow et al. [4]. Most importantly we found that 3-, 4- and 5-photon absorption are all present at levels that can affect devices that require a strong nonlinear response, such as those used for supercontinuum generation.

Because multi-photon absorption is always associated with the creation of free carriers whose absorption increases in proportion to λ^2, damaging levels of nonlinear absorption are more likely when using long (10 ps) laser pulses which accumulate large numbers of free carriers during the pulse. Femtosecond pulses are less affected by free carriers and, hence, offer the possibility of larger nonlinear response due to lower total absorption, at least in devices where the dispersion is normal. When the dispersion is anomalous things become more complicated because soliton pulse compression can increase the local intensity enhancing the nonlinear loss.

In the context of the successful experiments reported by Kuyken et al. [12] and Lamont et al. [13] on mid-IR SC generation, we note that Kuyken et al. used shorter pulses than those used in the experiments in section 2, and also a wavelength and waveguide where the nonlinear parameter was very much larger than at 3.55 μm. Furthermore, operating at 2.15 μm corresponds to the transition region between 2PA and 3PA which by analogy with the trends shown in Fig. 8 should be a "sweet spot" where the nonlinear absorption is small relative to that at either shorter or longer wavelengths. At 2.15 μm the effect of FCA is also reduced.

In the work by Lamont et al. [13] ultrashort pulses were used and as we have shown these minimise FCA. Additionally at 2.5 μm the waveguide nonlinear parameter should also be significantly larger than at 3.55 μm due to an increasing n_2 and the inverse dependence of the nonlinear parameter on wavelength. Thus, it appears these experiments were also performed in conditions where nonlinear absorption was relatively small. However, according to the results presented here, even a quite small change in the experimental parameters could change this drastically.

To conclude we emphasise that it is not safe to assume that nonlinear absorption in always negligible in silicon photonic devices operating in the mid-IR particularly if a strong nonlinear response is required ($F \gg \pi$). Careful attention should be paid to experimental parameters such as the pulse duration and wavelength of the pump source to minimise the impact of nonlinear absorption. In addition long (2-3 cm) low loss (<1dB/cm) devices are key to achieving large nonlinear optical response at the lowest possible intensity which can mitigate nonlinear loss.

Acknowledgements. Yi Yu acknowledges the financial support from the China Scholarship Council for her PhD Scholarship No. 201206110048. This research was conducted by the Australian Research Council Centre of Excellence for Ultrahigh Bandwidth Devices for Optical Systems (project number CE110001018). Support for this work was also provided by the FP7-ERC-MIRACLE project.

Received: 17 July 2013, **Revised:** 12 September 2013, **Accepted:** 16 September 2013

Published online: 17 October 2013

Key words: Silicon photonics, nonlinear, mid-infrared, multi-photon absorption.

References

[1] B. Jalali and S. Fathpour, J. Lightwave Technol. **24**(12), 4600–4615 (2006).

[2] J. Leuthold, C. Koos, and W. Freude, Nature Photon. **4**(8), 535–544 (2010).
[3] M. C. Estevez, M. Alvarez, and L. M. Lechuga, Laser Photon. Rev. **6**(4), 463–487 (2012).
[4] A. D. Bristow, N. Rotenberg, and H. M. van Driel, App. Phy. Lett. **90**(19), 191104 (2007).
[5] Q. Lin, J. Zhang, G. Piredda, R. W. Boyd, P. M. Fauchet, and G. P. Agrawal, App. Phy. Lett. **91**(2), 021111 (2007).
[6] D. Dimitropoulos, R. Jhaveri, R. Claps, J. Woo, and B. Jalali, App. Phy. Lett. **87**(7), 071115 (2005).
[7] M. Waldow, T. Pltzing, M. Gottheil, M. Frst, J. Bolten, T. Wahlbrink, and H. Kurz, Opt. Exp. **16**(11), 7693–7702 (2008).
[8] A. Turner-Foster, M. Foster, J. Levy, C. Piotras, R. Salem, A. Gaeta, and M. Lipsom, Opt. Exp. **18**(4), 3582–3591 (2010).
[9] A. Gajda, L. Zimmermann, M. Jazayerifar, G. Winzer, H. Tian, R. Elschner, T. Richter, C. Schubert, B. Tillack, and K. Petermann, Opt. Exp. **20**(12), 13100–13107 (2012).
[10] M. Dinu, F. Quochi and H. Garcia, App. Phy. Lett. **82**(18), 2954–2956 (2003).
[11] S. Pearl, N. Rotenberg, and H. M. van Driel, App. Phy. Lett. **93**(13), 131102 (2008).
[12] B. Kuyken, X. P. Liu, R. M. Osgood, R. Baets, G. Roelkens, and W. M. J. Green, Opt. Exp. **19**(21), 20172–20181 (2011).
[13] M. R. Lamont, R. K. Lau, A. Griffith, Y. H. Wen, Y. Okawachi, M. Lipson, and A. L. Gaeta, Mid-infrared su- percontinuum generation in silicon waveguides, OSA Tech-nical Digest (online) (Optical Society of America, 2013), p. CW3H.1.
[14] M. Muneeb, X. Chen, P. Verheyen, G. Lepage, S. Pathak, E. Ryckeboer, A. Malik, B. Kuyken, M. Nedeljovic, J. V. Campenhout, G. Mashanovich, and G. Roelkens, Opt. Exp. **21**(10), 11659–11669 (2013).
[15] V. Z. Kolev, M. W. Duering, B. Luther-Davies, and A. V. Rode, Opt. Exp. **14**(25), 12302–12309 (2006).
[16] X. Gai, D. Y. Choi, S. Madden, Z. Y. Yang, R. P. Wang, and B. Luther-Davies, Opt. Lett. **37**(18), 3870–3872 (2012).
[17] X. Z. Sang, E. K. Tien, and O. Boyraz, J. Opt. Adv. Mat. **11**(1), 1–25 (2008).
[18] D. K. Schroder, R. N. Thomas, and J. C. Swartz, IEEE Journal of Solid-State Circuits **13**(1), 180–187 (1978).
[19] P. P. Pronko, P. A. VanRompay, C. Horvath, F. Loesel, T. Juhasz, X. Liu, and G. Mourou, Phy. Rev. B **58**(5), 2387–2390 (1998).
[20] A. Vaidyanathan, T. W. Walker, and A. H. Guenther, IEEE J. Quantum Electron. **16**(1), 89–93 (1980).
[21] S. J. Madden, D. Y. Choi, D. A. Bulla, A. V. Rode, B. Luther-Davies, V. G. Ta'eed, M. D. Pelusi, and B. J. Eggleton, Opt. Exp. **15**(22), 14414–14421 (2007).
[22] Y. Choi, J. H. Park, M. R. Kim, W. Jhe, and B. K. Rhee, App. Phy. Lett. **78**(7), 856–858 (2001).
[23] M. Sheik-Bahae, A. A. Said, T. H. Wei, D. J. Hagan, and E. W. Van Stryland, IEEE J. Quantum Electron. **26**(4), 760–769 (1990).
[24] M. Dinu, IEEE J. Quantum Electron. **39**(11), 1498–1503 (2003).
[25] D. S. Correa, L. De Boni, L. Misoguti, I. Cohanoschi, F. E. Hernandez, and C. R. Mendonca, Opt. Commun. **277**(2), 440–445 (2007).
[26] B. S. Wherrett, J. Opt. Soc. Am. B., Opt. Phy.. **1**(1), 67–72 (1984).
[27] T. Boggess, K. Bohnert, K. Mansour, S. C. Moss, I. Boyd, and A. Smirl, IEEE J. Quantum Electron. **22**(2), 360–368 (1986).
[28] D. K. Schroder, R. N. Thomas, and J. C. Swartz, IEEE Journal of Solid-State Circuits **13**(1), 180–187, (1978).
[29] K. B. Svantesson, Journal of Physics-**D12**, 425–436, (1979).
[30] A. Cutolo, M. Iodice, P. Spirito, and L. Zeni, J. Lightwave Techn. **15**(3), 505–518, (1997).